Thermodynamic Variability within the Convective Boundary Layer Due to Horizontal Convective Rolls

TAMMY M. WECKWERTH

Department of Atmospheric Sciences, University of California at Los Angeles, Los Angeles, California, and Advanced Study Program, National Center for Atmospheric Research, Boulder, Colorado*

JAMES W. WILSON

National Center for Atmospheric Research, Boulder, Colorado*

ROGER M. WAKIMOTO

Department of Atmospheric Sciences, University of California at Los Angeles, Los Angeles, California

(Manuscript received 15 February 1995, in final form 6 September 1995)

ABSTRACT

Data from the Convection and Precipitation/Electrification (CaPE) Experiment conducted during the summer of 1991 are used to examine and quantify the horizontal variability of temperature and moisture within the convective boundary layer (CBL). Potential temperature variations were only about 0.5 K, while variations in water vapor mixing ratio values of 1.5–2.5 g kg^{-1} were observed throughout the CBL. Using radar, aircraft, and sounding data, it is shown that horizontal convective rolls are the likely cause of these variabilities. The enhanced moisture occurred within the roll updraft regions, thus rolls were transporting moist air from the surface upward. The observed cloud-base heights, obtained from cloud photogrammetry, were produced from the highest moisture values within the roll updraft regions. Since the roll ascending branches contained moisture values that were most representative of the observed cloud-base heights, it is likely that measurements from within the roll updrafts would provide the best estimate of the potential for deep, moist convection.

1. Introduction

Horizontal convective rolls are counterrotating horizontal vortices that have been predicted with theory (e.g., Asai 1970, 1972; Kuettner 1971; Brown 1980), studied in the laboratory (e.g., Krishnamurti 1975; Faller 1965; Deardorff et al. 1980), simulated with numerical models (e.g., Sun 1978; Sykes and Henn 1989; Moeng and Sullivan 1994) and observed within the CBL (e.g., Malkus and Riehl 1964; LeMone 1973; Kelly 1982, 1984). They commonly occur over uniform terrain when there is a moderate surface heat flux and when some minimum wind speed or vertical wind shear value is achieved (e.g., Woodcock 1942; Kropfli and Kohn 1978; Grossman 1982). Previous observational studies have shown that the ascending and descending branches of rolls provide an efficient means of vertically transporting heat and moisture across the CBL (e.g., LeMone 1973, 1976; LeMone and Pennell 1976; Brümmer 1985; Chou and Ferguson 1991; Crook 1991; Kristovich 1991). They showed that throughout the lowest 70%–80% of the CBL, the ascending branches of the rolls carry upward the warm, moist air that originated at the surface. Within the top portion of the CBL and within the capping inversion, the descending branches of the rolls tend to carry downward the warm, dry air originating within the inversion.

The vertical transport within the roll updraft and downdraft regions has been shown to cause varying magnitudes of horizontal variability of heat and moisture. LeMone and Pennell (1976) examined clear-air rolls within 100 m beneath cloud base. They noted that the temperature decreased approximately 0.1 K and the vapor density increased 0.5 g m^{-3} within the roll updraft regions. In another study of clear-air rolls, Reinking et al. (1981) observed increases of 0.5 K in potential temperature and decreases of 3.5 g m^{-3} in vapor density within the roll downdraft regions at $0.67z_i$, where z_i is the height of the inversion base. Atlas et al. (1986) examined data at two flight levels taken across rolls that existed during a cold-air outbreak event. At

* The National Center for Atmospheric Research is partially sponsored by the National Science Foundation.

Corresponding author address: Dr. Tammy M. Weckwerth, NCAR/Advanced Study Program, P.O. Box 3000, Boulder, CO 80307-3000.
E-mail: tammy@ucar.edu

$0.26z_i$ they found that the updrafts were 0.5 K warmer and 0.5 g m^{-3} more moist than the surrounding air. At the base of the inversion, however, the variability was larger wherein the downdrafts were 3 K warmer and 0.8 g m^{-3} drier. All of these studies resulted in similar findings, even though they had aircraft data from only one or two heights. Kristovich (1991) was able to examine the variability at several heights within rolls that occurred during a lake-effect snowstorm. The variability within these rolls, however, was much less than in previous studies. He found that throughout approximately 80% of the CBL, the roll updrafts were generally 0.15 K warmer and 0.08 g m^{-3} more moist. The lack of large variability with the lake-effect snowstorm rolls may have been due to the relatively higher environmental shear, which likely caused enhanced mixing of the CBL. Another explanation may be due to the increased mixing caused by the relatively deeper convection associated with the lake-effect snowstorms.

Thermodynamic variability due to rolls was also shown to occur with numerical model simulations (e.g., Crook 1991; Moeng and Sullivan 1994). A modeling forecast application of this variability was performed by Crook (1991). During a field project in Colorado he used the Clark (1977) numerical cloud model to predict thunderstorm formation. The simulation was initialized with a local sounding and it produced a null forecast. One-half hour later, however, the radar data indicated that thunderstorms formed. Upon closer examination of the day, Crook (1991) noted that rolls existed at the time of the sounding launch. He suspected that the sounding was launched in a relatively dry portion of the rolls and noted that by increasing the dewpoint temperature by 1–2 K it would change his model forecast from null to the prediction of 50-dBZ storms.

Similar variability in CBL horizontal moisture and temperature measurements has been observed with frontal zones (e.g., Palmén and Newton 1977) and stationary boundaries (e.g., Wilson et al. 1992). This study, however, focuses on the variability and forecasting issues due to the special case of horizontal convective rolls. These analyses are unique in that they combine aircraft, sounding and radar data to examine the detailed thermal and moisture variability throughout the CBL during clear-air roll occurrences. In addition, cloud photogrammetry provides for a direct measurement of the cloud-base heights produced by the roll updraft regions. This paper will focus on the horizontal moisture variations on three days by 1) providing evidence that the observed variations are caused by rolls at several levels throughout the entire CBL, as well as quantifying those variations, and 2) describing the effect of the variability upon the estimate of the potential for deep, moist convection.

A discussion of the observational platforms used in these analyses is provided in section 2. Evidence of the existence of rolls is presented in section 3. Utilizing sounding and aircraft data, section 4 shows that the rolls caused horizontal thermodynamic variability throughout the entire CBL. Section 5 examines the effects of the variability on the estimates of the potential for deep, moist convection. A summary and conclusions are presented in section 6.

2. Observational platforms

Wakimoto and Atkins (1994) provided a discussion of the observational platforms used for these analyses, as well as a base map of the CaPE project area (see their Fig. 1). Of primary importance in this paper are the National Center for Atmospheric Research's (NCAR) CP3 and CP4 Doppler radars, CLASS (Cross-chain Loran Atmospheric Sounding System) soundings, PAM II (Portable Automated Mesonet II) surface stations, cloud photographs, and the NCAR King Air and the University of Wyoming (UW) King Air research aircraft.

The radar data were edited to remove ground clutter and second-trip echoes with the Research Data Support System (RDSS) software package (Oye and Carbone 1981). Comparisons between radar and aircraft data were made after interpolating the radar data onto a Cartesian grid using a grid spacing of 250 m with the Cressman (1959) interpolation scheme. The interpolated data were displayed with the CEDRIC [custom editing and display of reduced information in Cartesian space; Mohr and Miller (1983)] software package.

The aircraft data required significant corrections. The NCAR King Air often exhibited an inaccurate position reading of as much as 5 km due to INS (Inertial Navigation System) errors. Therefore, the backscatter from the aircraft detected by the CP3 and CP4 radars was used to determine the location of the aircraft. The horizontal position absolute accuracy using this technique was approximately 300 m. The UW King Air data had previously been corrected for INS position errors and for errors caused by the Schuler oscillation with the procedure described in Rodi et al. (1991). The backscatter return detected by the radars always confirmed the UW King Air's recorded horizontal position. The vertical positions of both aircraft were obtained by converting the measured static pressure field to altitude using a nearby sounding. The resulting absolute accuracy of the aircraft altitude was about 100 m. The moisture, measured by a frost-point hygrometer, and vertical velocity data from the UW King Air were corrected for known biases obtained from intercomparison flights with the NCAR King Air and tower flybys during CaPE in a manner described by Fankhauser et al. (1985). This correction required a subtraction of 0.95 g kg^{-1} and 0.3 m s^{-1} for the respective UW King Air mixing ratio and vertical velocity measurements. After all corrections were made, the expected absolute accuracies (precisions) of the aircraft mixing ratio and potential temperatures used in these analyses were 0.4 g kg^{-1}

(0.04 g kg^{-1}) and 0.4 K (0.04 K), respectively [quoted by the Research Aviation Facility (RAF) of NCAR in Kessinger (1988)]. All of the corrections, as well as objective analyses procedures, were performed with the ACANAL (aircraft data processing and objective analysis of aircraft tracks) software package (Fankhauser et al. 1985).

Corrections for the response time of the temperature and moisture sensors of the CLASS soundings in the CBL were also made. Throughout the lowest 1 km of the sonde's ascent it is suspected that the temperature sensor was reading a value too high due to solar heating and lack of ventilation before launch. This produced a relative humidity reading that was too low. Therefore, a correction was made to adjust for the thermal lag of the sensor (Miller and Riddle 1994). This correction is discussed further in the appendix. The absolute accuracies (precisions) of the measurements within the CBL were approximately 1.5 g kg^{-1} (0.4 g kg^{-1}) and 0.5 K (0.2 K) for mixing ratio and potential temperature, respectively (Mueller et al. 1993; Martner et al. 1993).

PAM II surface station data were utilized for the surface measurements. The temperature and moisture measurements were obtained at 2 m AGL, while the winds were measured at 10 m AGL.

The heights of cloud bases and tops in photographs taken from the CP3 radar site were determined from photogrammetric techniques (e.g., Holle 1986; Kingsmill and Wakimoto 1991). An azimuth–elevation grid was placed upon the photographs and the range to each cloud was obtained from the CP3 radar. The resulting cloud-base heights are estimated to be accurate to within 50 m.

3. Evidence of rolls

This section will describe the large-scale conditions on the three days to be examined in detail. It will also show that the dominant form of boundary layer convection was rolls. Cloud streets, which are readily apparent in the satellite imagery, are known to be associated with horizontal convective roll motions within the CBL (e.g., LeMone and Pennell 1976). The linear patterns of the radar reflectivity field are also used to confirm the existence of rolls (e.g., Christian and Wakimoto 1989).

a. Satellite data

The visible satellite imagery at 1700 UTC (hereafter all times will be UTC; UTC = EDT + 4 h) on 17 August 1991 is shown in Fig. 1a. Tropical Storm Bob was east of Florida and the storm's rainbands were never closer than 50 km from the CaPE region (shown by an arrow in Fig. 1a). The tropical storm induced subsidence over the Florida peninsula likely inhibiting the growth of deep convection. In addition, it created the northwesterly flow regime apparent from the PAM wind directions and the cloud street orientation. The correspondence between surface wind direction and cloud street orientation is consistent with observations by Malkus and Riehl (1964). Other than determining the orientation of the roll axes, it is believed that the tropical storm did not affect the CBL motions. Note the somewhat discrete nature of the small cumulus clouds along the cloud streets, a feature termed "pearls on a string" by Kuettner (1959).

At 1700 on 2 August 1991 the center of the Bermuda high was located southeast of Florida thereby causing a turning of the winds over the peninsula. Note that in the southern portion of Fig. 1b, the cloud streets were aligned more nearly north–south, as compared with the cloud streets over the CaPE network that were oriented northeast–southwest. Once again these orientations were roughly parallel to the surface wind directions.

On 10 August the center of the Bermuda high was located south of Florida, which created the westerly flow shown by the surface stations and the east–west cloud streets over eastern Florida (Fig. 1c). At 1700 deep convection initiated by Florida's west coast seabreeze front was occurring over the western portion of the peninsula.

b. Radar data

The radar reflectivity and Doppler velocity from CP3 radar (see Fig. 1 for location) at 1715 on 17 August are shown in Fig. 2. Note that the northwest–southeast linear patterns in radar reflectivity (i.e., alternating yellow and green bands) correspond to the orientation of the cloud streets (Fig. 1a). The linear radar reflectivity enhancements, or fine lines, indicate the roll updraft regions (Christian and Wakimoto 1989) due to a concentration of insects into the low-level convergence zones as they resisted ascent into colder surroundings (Achtemeier 1991; Wilson et al. 1994). The Doppler velocity field shows that the mean wind direction was northwesterly (Fig. 2b), the same as the fine-line orientation. There is also a suggestion of alternating bands of confluence and diffluence caused by the roll circulations (Kelly 1982). Although not well-defined, the alternating pattern of yellow and green is most apparent near the zero velocity regions (i.e., along the 240° azimuth).

At 1645 on 2 August an RHI (range–height indicator) scan nearly perpendicular to the roll axes shows the low-level enhancements of radar reflectivity every 2–4 km likely due to the roll updrafts (Fig. 3a). Small cumulus clouds occurred atop many of the low-level reflectivity enhancements. The relatively low reflectivity values near the surface were caused by intervening trees blocking the radar beam. The black arrows indicate the low-level convergence zones corresponding with many of the reflectivity maxima (Fig. 3b). Cloud-top divergence was also evident in a few cases, partic-

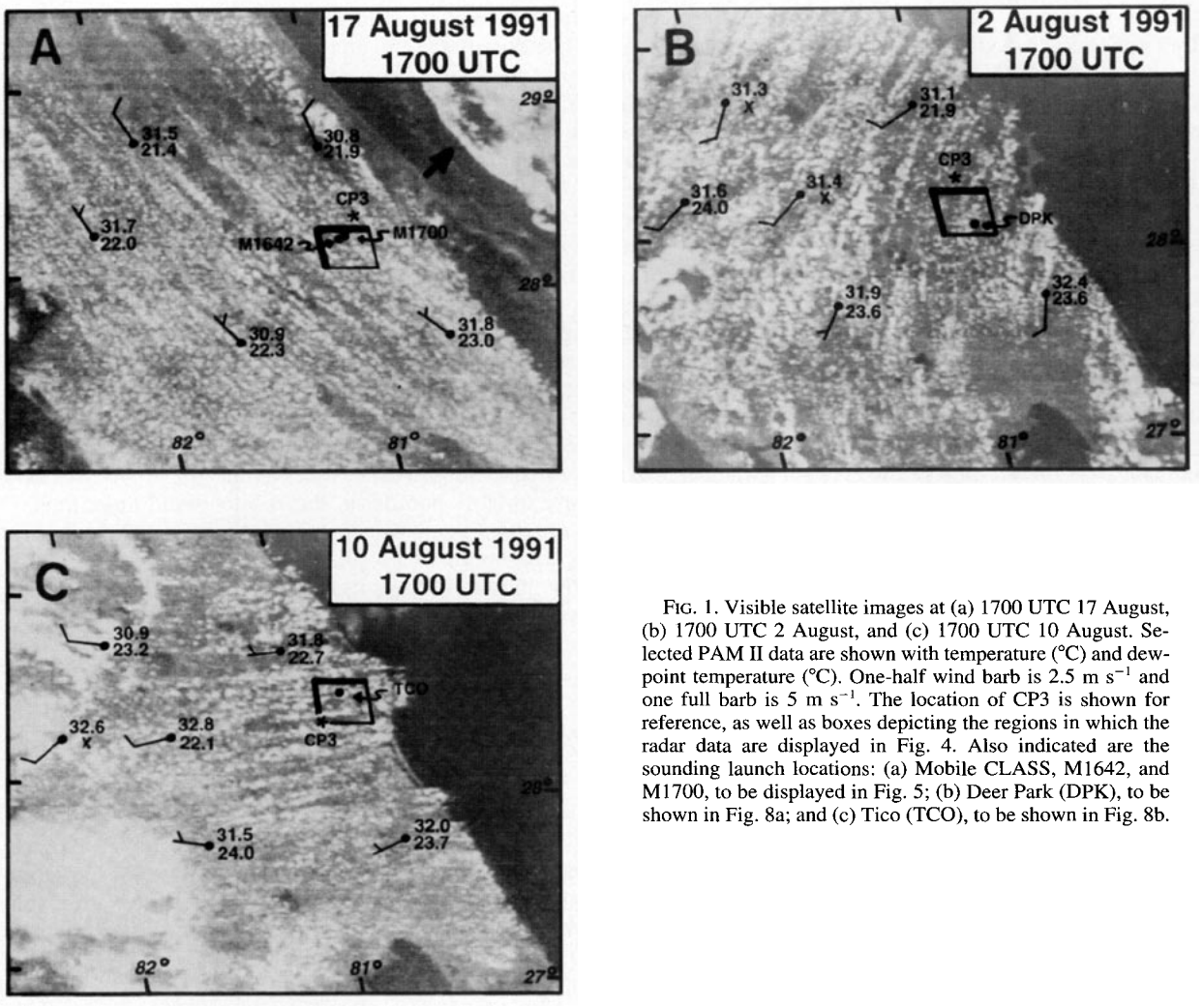

FIG. 1. Visible satellite images at (a) 1700 UTC 17 August, (b) 1700 UTC 2 August, and (c) 1700 UTC 10 August. Selected PAM II data are shown with temperature (°C) and dewpoint temperature (°C). One-half wind barb is 2.5 m s^{-1} and one full barb is 5 m s^{-1}. The location of CP3 is shown for reference, as well as boxes depicting the regions in which the radar data are displayed in Fig. 4. Also indicated are the sounding launch locations: (a) Mobile CLASS, M1642, and M1700, to be displayed in Fig. 5; (b) Deer Park (DPK), to be shown in Fig. 8a; and (c) Tico (TCO), to be shown in Fig. 8b.

ularly the clouds at 23 and 39 km. Figure 3 shows that the clouds atop the CBL were generally associated with the roll updraft regions. Similar findings were obtained by LeMone and Pennell (1976) and Christian and Wakimoto (1989). There are some cases in which this was not true. For example, the cloud at 23 km appears to be displaced to the right from the CBL reflectivity maximum simply because this RHI did not pass through the cloud center that was likely directly atop the low-level reflectivity maximum. The cloud at 34 km was not directly above the CBL reflectivity maximum since it was dissipating.

The CP3 interpolated reflectivity field at 1643 on 17 August within the box of Fig. 1a is shown in Fig. 4a. Just as in Figs. 1a and 2a, the roll updraft regions were fairly well defined and linear. Two mobile CLASS soundings were launched to examine the rolls: one at 1642 (hereby called M1642) and one at 1700 (M1700). The launch positions were shown in Fig. 1a, as well as in Fig. 4a, along with the balloon ascent tracks of the lowest 2 km. The ascent track of M1700 was adjusted for roll motion since it was launched 18 min after the time of the radar display shown. The ascent track of M1642 coincided with a fine line as it propagated along the mean CBL wind direction, which is suggestive that it ascended through a roll updraft region.

At 1650 on 2 August the roll axes were northeast–southwest (Fig. 4b), just as shown by the cloud-street orientation within the box of Fig. 1b. The corresponding sounding was launched from the Deer Park (DPK) site at 1650 and its ascent track throughout the lowest 2 km is indicated. Note that the sounding was launched nearby but not within a reflectivity enhancement, suggesting that it was not released into the updraft portion of a roll. The UW King Air cross-roll flight track is shown. The NCAR King Air was flying directly above the UW King Air. The dots and letters along the flight track indicate points at which the aircraft crossed fine lines

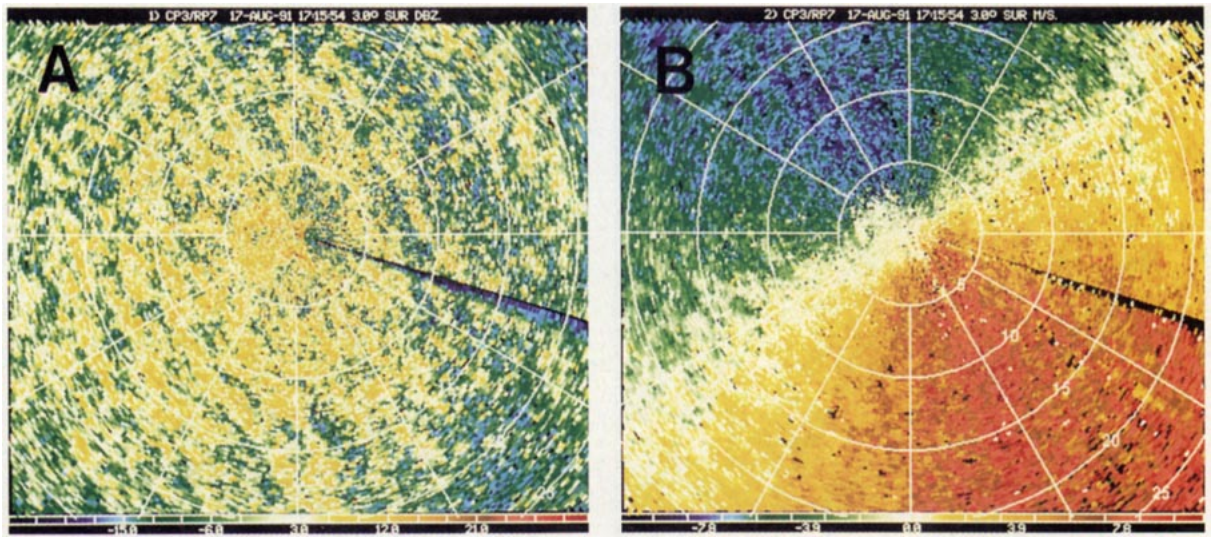

FIG. 2. CP3 surveillance scan from 3° at 1715 UTC 17 August showing (a) reflectivity (dBZ_e) and (b) Doppler velocity ($m\ s^{-1}$). Corresponding scales are beneath each panel. Range rings are every 5 km and azimuth lines are every 30°.

likely caused by roll updrafts. These locations will be useful when examining the time series of aircraft data in section 4b.

At 1700 on 10 August the rolls were not well defined but there was a definite east–west linearity to the convective motions (Fig. 4c) within the box of Fig. 1c.

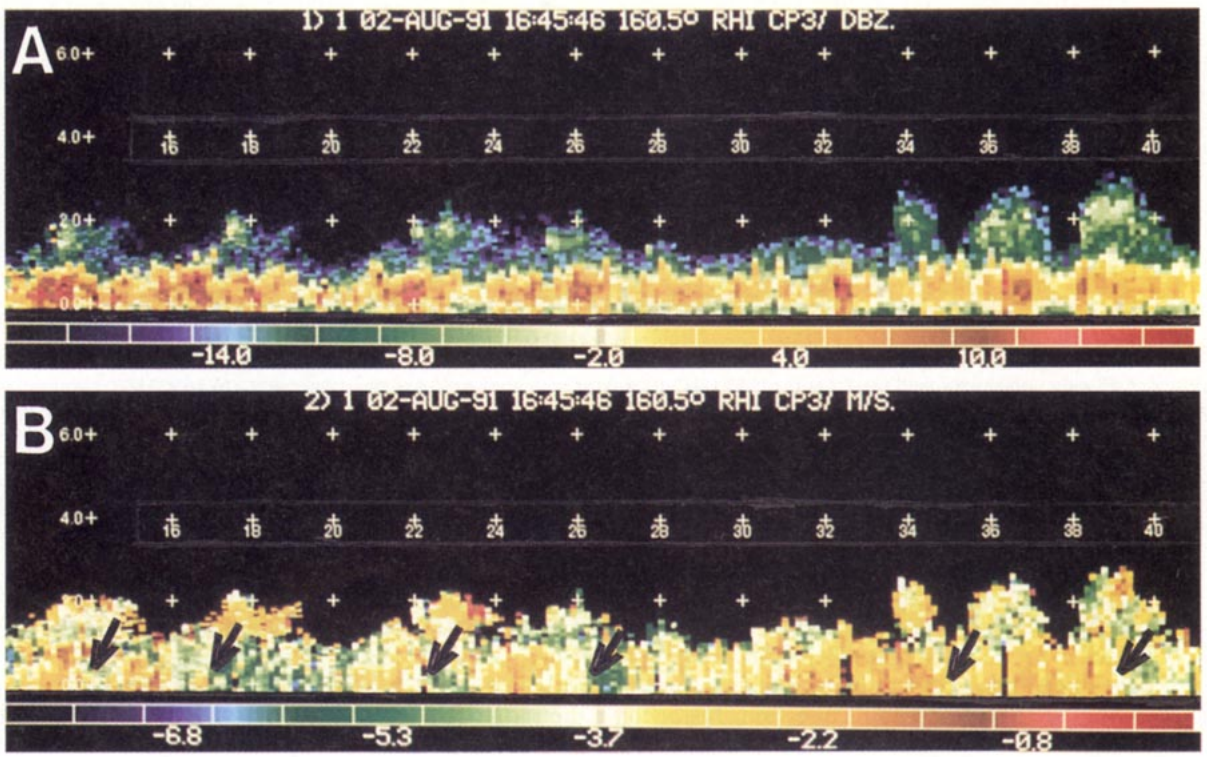

FIG. 3. CP3 RHI scan nearly perpendicular to the roll axes at 1645 UTC 2 August showing (a) reflectivity (dBZ_e) and (b) Doppler velocity ($m\ s^{-1}$). Arrows mark the locations of low-level convergence due to the roll updraft regions. Corresponding scales are beneath each panel. Tick marks are every 2 km.

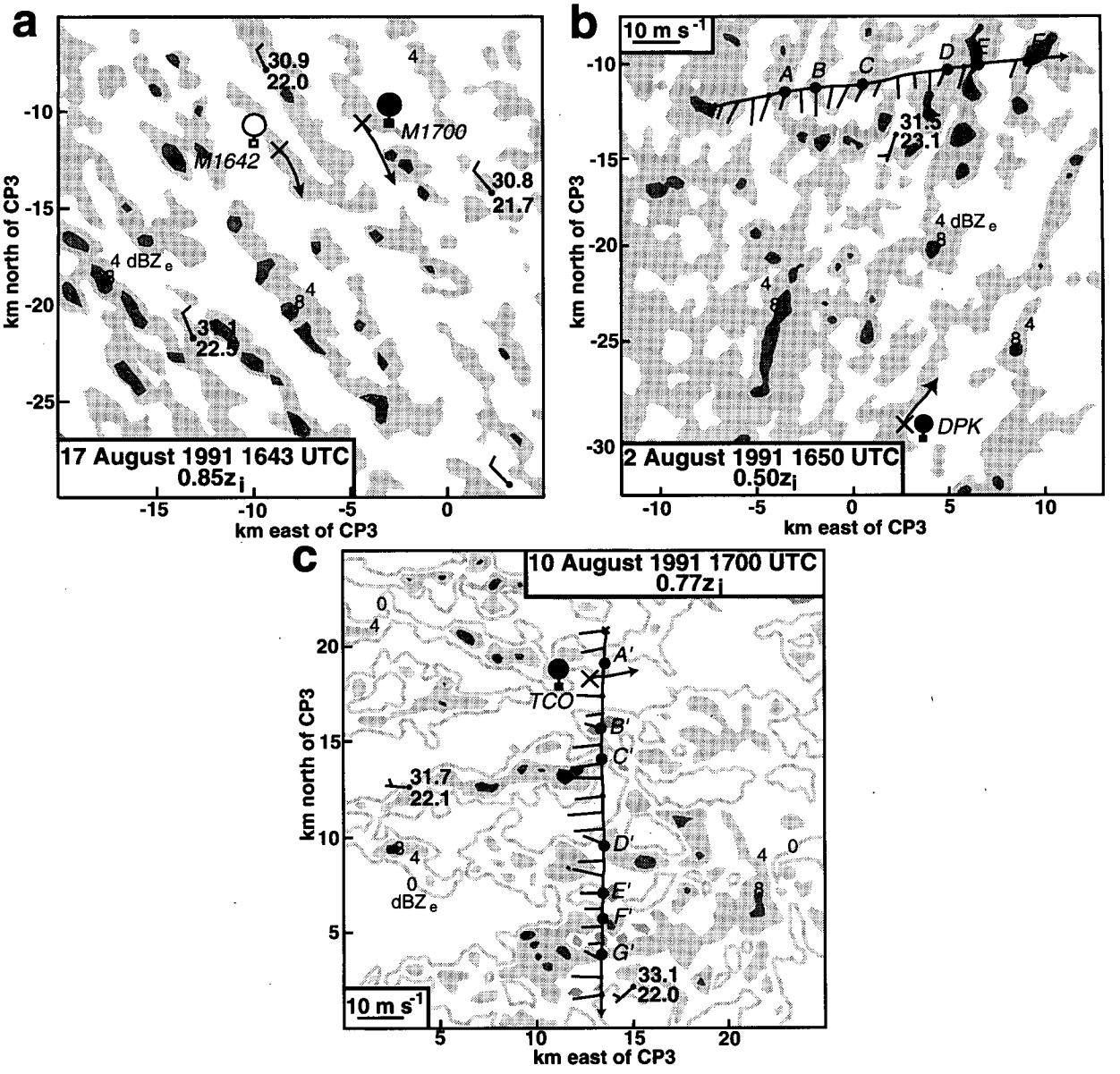

FIG. 4. CP3 radar reflectivity field (dBZ_e) at (a) 1643 UTC 17 August with northwest–southeast fine lines, (b) 1650 UTC 2 August with northeast–southwest fine lines, and (c) 1700 UTC 10 August with east–west fine lines. Reflectivity values greater than 4 dBZ_e are lightly shaded and those greater than 8 dBZ_e are darkly shaded. The 0-dBZ_e contour is also included in (c). The regions displayed are shown by the boxes in Fig. 1. Several PAM II station data points are plotted on each panel, as in Fig. 1. The sounding ascent trajectories, adjusted for roll motion, are indicated. The length of each trajectory is 2 km vertical distance. In (b) and (c) the UW King Air flight tracks are also shown. Letters indicate locations at which the aircraft crossed radar reflectivity maxima and will be used in Fig. 6. The 10 m s^{-1} lines indicate the scales of the aircraft-measured winds.

The sounding, released from Tico Airport (TCO), was likely launched between the updraft and downdraft portions of the rolls. The aircraft actually flew directly over the sounding site in the cross-roll direction. Just as on 2 August, they were flying in a stacked formation.

The respective roll wavelengths, measured from both the cloud streets and radar reflectivity enhancements, on 17, 2, and 10 August were approximately 3, 3, and 5 km. The corresponding CBL depths were 1.0, 1.2, and 1.1 km, thereby producing roll aspect ratios of 3.0, 2.5, and 4.6. These values were within the range of previous roll observations (e.g., Kuettner 1971; LeMone 1973; Weston 1980; Atlas et al. 1983).

The existence of rolls at 1700 on all three days was apparent from 1) the occurrences of cloud streets, 2)

the relatively linear orientations of the fine lines of reflectivity along the wind direction, and 3) the aspect ratios which compared well with previous research on rolls. The effect that these rolls had on the horizontal thermal and moisture fields will be examined presently.

4. Thermodynamic variability due to rolls

a. Sounding data

The two soundings launched on 17 August are compared in Fig. 5. The schematic diagram in the center of the figure depicts a vertical cross section of the relative locations of the launches within the roll circulations. M1642, which was likely launched into a roll updraft, is shown by the white balloon and thick lines on the sounding while M1700, launched between an updraft and downdraft of rolls, is shown by the black balloon and relatively thin lines. The ascent rate for both balloons is shown on the left of Fig. 5. Within the CBL, M1642 ascended at 7–9 m s^{-1}, while M1700 ascended at only 4–6 m s^{-1}, providing evidence that M1642 was launched into a roll updraft region. The ascent rate of M1642 increased to about 10 m s^{-1} between 1.5 and 2 km. This was likely caused by the sonde experiencing an increased updraft during a cloud penetration. Above 2 km, the ascent rates were fairly uniform.

There was not much variation between the two soundings in the temperature profile; potential temperature was well mixed throughout the CBL. This is consistent with the small potential temperature variabilities shown in previous studies during roll occurrences. The horizontal wind speeds were also comparable for both soundings.

The primary difference between the two soundings within the CBL was the moisture profile. M1642 measured approximately 1.5 g kg^{-1} more moisture than M1700 throughout the entire depth of the CBL. The thermodynamics of M1642 support the suggestion of the ascent rate that the sonde penetrated a cloud at 1.5 km AGL. The temperature increased and the air was nearly saturated, therefore a cloud is shown schematically within the 500-m layer. When M1642 exited the cloudy region, the temperature sensor was likely wet and, as a result of evaporation from the sensor, measured a value colder than actual, thereby recording a false superadiabatic lapse rate. The fact that M1642 went through a cloud is more evidence that the sounding was launched into a roll updraft since it has been shown that the clouds occur atop roll updraft regions (Fig. 3a). The moisture difference above the CBL was also observed with aircraft data on several other days (not shown). This may be a result of internal gravity waves (i.e., convection waves) aloft (e.g., Kuettner et al. 1987). It seems as if the enhanced moisture variability in this example was due to the roll updraft regions. In order to examine the variability with more detail, aircraft data is necessary. It was not available on 17 August, but 2 and 10 August both had several flight tracks within and atop the CBL. These aircraft data will be used to further explore the possibility that the CBL moisture variability was caused by rolls throughout the depth of the CBL, as well as to quantify that variability.

b. Aircraft data

Figure 6 shows in situ aircraft data and CP3 radar reflectivity. On 2 August the NCAR King Air was fly-

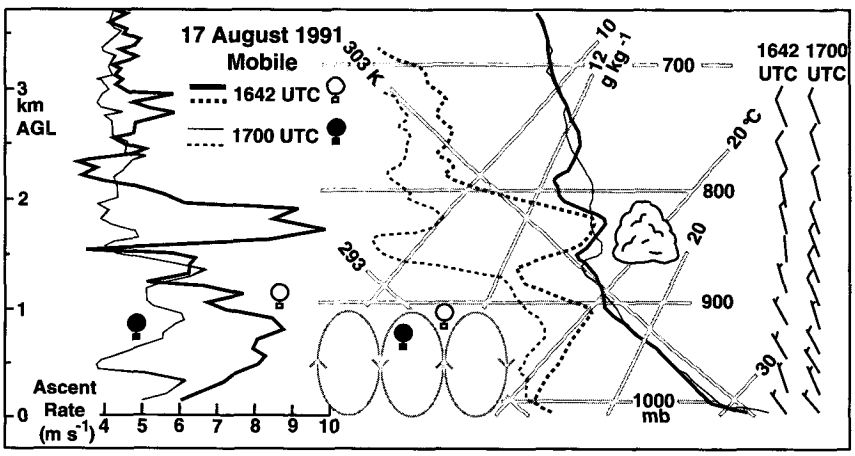

FIG. 5. Mobile CLASS sounding comparisons taken on 17 August within the roll updraft region (1642 UTC called M1642 in the text; thick lines) and between a roll updraft and downdraft (1700 UTC called M1700 in the text; thin lines). These balloon launch locations are shown schematically in the center relative to the boundary layer roll circulations. See Fig. 4 for exact launch locations relative to radar reflectivity field. Schematic cloud indicates cloud penetration by M1642. The ascent rates (m s^{-1}) for each sonde are shown on the left. Horizontal wind speeds are shown on the right (full barb—5 m s^{-1}; half barb—2.5 m s^{-1}).

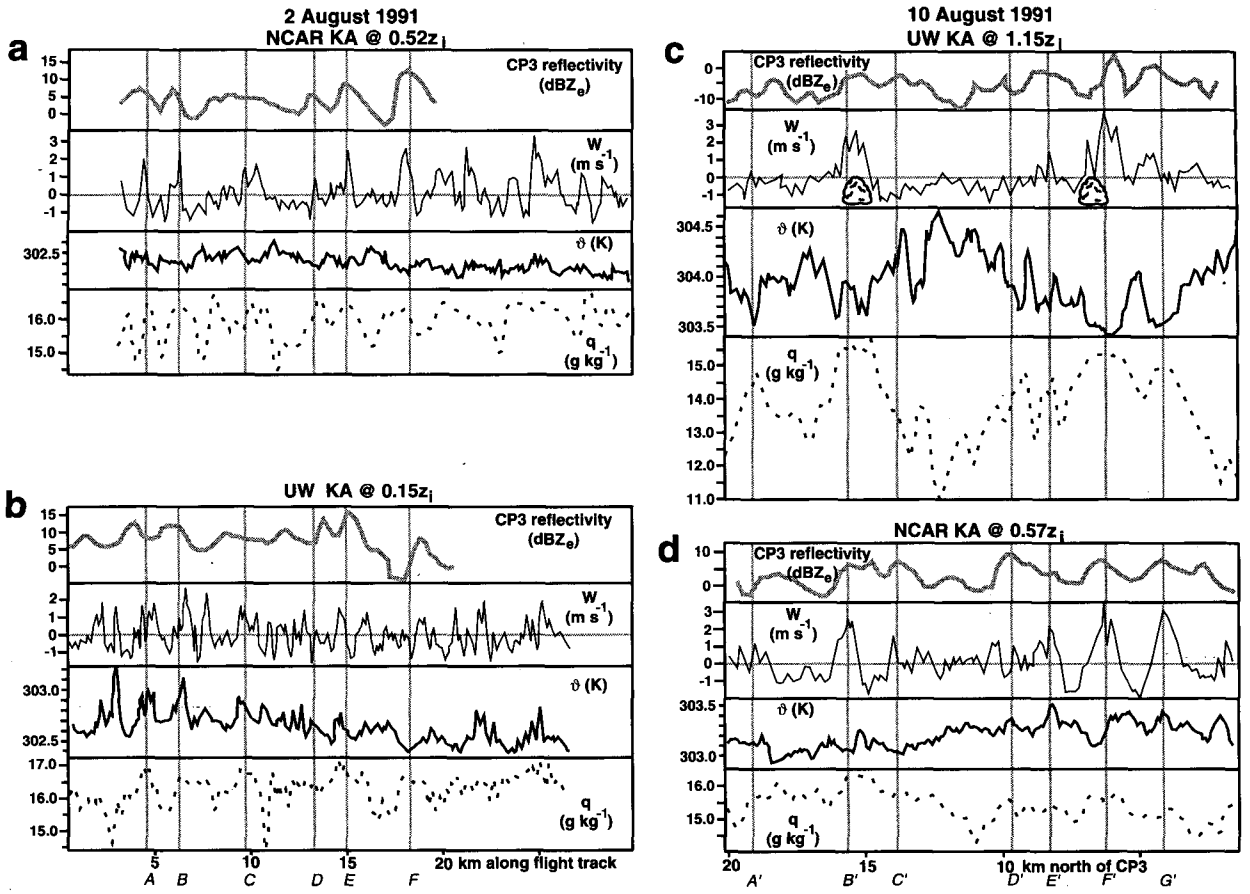

FIG. 6. Interpolated CP3 radar reflectivity (dBZ_e; gray line) and time series of aircraft-measured vertical velocity (m s^{-1}; thin solid line), potential temperature (K; thick solid line), and mixing ratio (g kg^{-1}; dashed line). Data from the (a) NCAR King Air at $0.52z_i$, (b) UW King Air at $0.15z_i$ on 2 August, (c) UW King Air at $1.15z_i$, and (d) NCAR King Air at $0.57z_i$ on 10 August are shown. Flight tracks for 2 and 10 August are shown in Figs. 4b and 4c, respectively. Letters correspond with locations of reflectivity maxima along the flight tracks of Fig. 4. Schematic clouds in (c) indicate times of cloud penetrations.

ing at $0.52z_i$ (624 m AGL) between 1650:00 and 1654:50 (Fig. 6a), while the UW King Air was flying beneath it at $0.15z_i$ (177 m AGL) between 1650:25 and 1655:00 (Fig. 6b). The top panel is the CP3 radar reflectivity along the track near the flight level. These data are plotted every 250 m (every 2.8 s along the flight track) and are terminated at the edge of the radar scan. The three lower panels show the 1-s aircraft-measured parameters. The same information is displayed for the UW King Air at $1.15z_i$ (1269 m AGL) between 1701:30 and 1706:40 (Fig. 6c) and the NCAR King Air at $0.57z_i$ (629 m AGL) between 1702:50 and 1706:40 on 10 August (Fig. 6d). The vertical lines with letter labels on the bottom correspond to the times at which the aircraft crossed the radar reflectivity maxima of Figs. 4b and 4c, which were likely representative of roll updraft regions.

In general, there was good agreement between the largest-amplitude (1–3 m s^{-1}), low-frequency (wavelengths of 2–5 km) updrafts and the enhanced radar reflectivity, indicating that the roll updrafts were exhibited as enhanced lines of radar reflectivity (Christian and Wakimoto 1989; Wilson et al. 1994). The exceptions were primarily found at $0.15z_i$ (Fig. 6b) where there were many small, high-frequency updrafts and downdrafts. This is consistent with results of LeMone (1976), who showed that turbulent eddies near the surface may be forced into more organized roll motions at higher levels. High-frequency fluctuations of vertical motion with magnitudes of about 0.5 m s^{-1} occurred on scales of less than 1 km at all levels and were likely due to turbulent eddies.

There was a tendency for the potential temperature and vertical velocity fields to be in phase near the surface (Fig. 6b), providing evidence that the rolls were a form of thermal convection (e.g., Kristovich 1991). Within the stable layer, however, there was a suggestion of an inverse relationship between updrafts and potential temperature maxima (Fig. 6c) such that the updrafts were forcing upward the relatively cool CBL

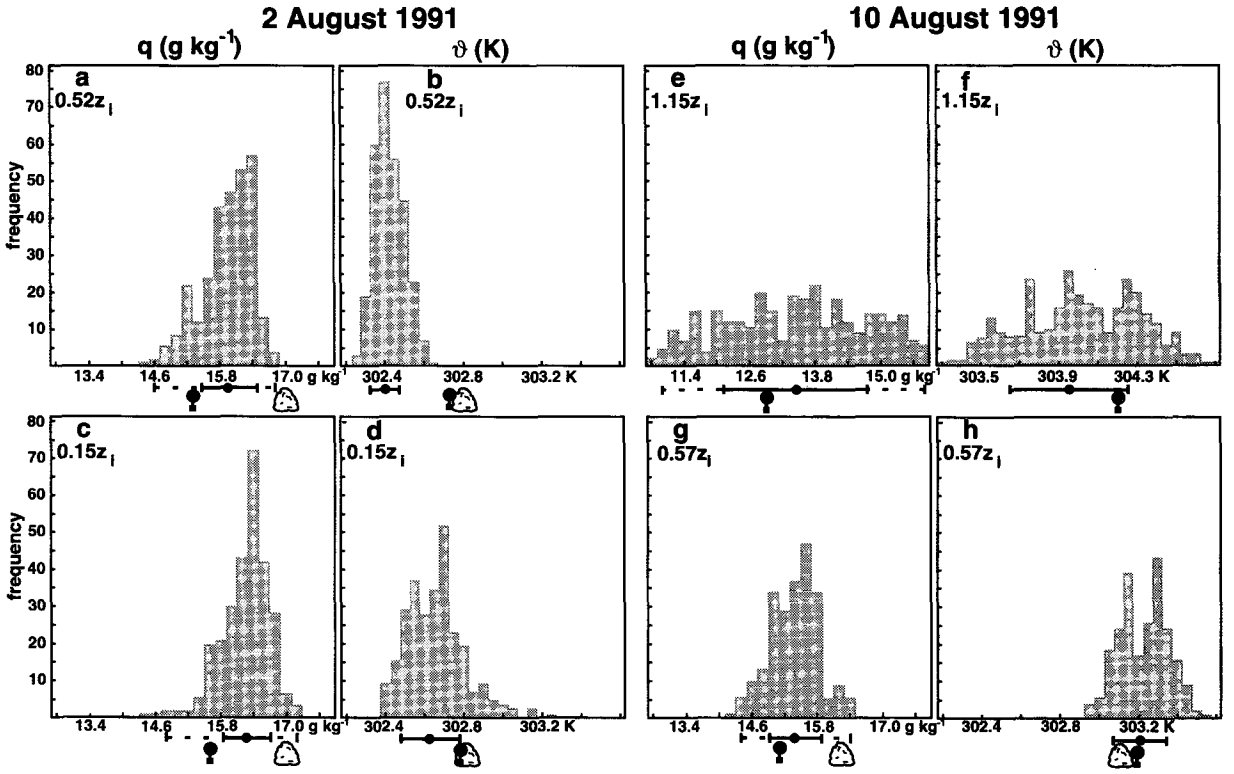

FIG. 7. Histograms of mixing ratio (g kg^{-1}; left columns for each day) and potential temperature (K; right columns for each day) measured by (a), (b) NCAR KA at $0.52z_i$ and (c), (d) UW KA at $0.15z_i$ on 2 August and (e), (f) UW KA at $1.15z_i$ and (g), (h) NCAR KA at $0.57z_i$ on 10 August. Aircraft means are shown by dots beneath each panel and one standard deviation is indicated by the solid lines. The range of data for mixing ratios is shown by dashed lines. Sounding symbols indicate 200-m sounding mean centered at the aircraft altitude. The cloud symbols indicate the value of each parameter necessary to create photogrammetric cloud base shown in Fig. 8. The cloud symbols are not shown for (e) and (f) since that flight leg was above cloud base.

air and the downdrafts were forcing downward the relatively warm stable-layer air. These results are similar to those of previous studies (e.g., LeMone 1973). The largest variations occurred nearest the surface (Fig. 6b) and within the stable layer (Fig. 6c), while the middle of the CBL was generally well mixed (Figs. 6a and 6d). Similar to that observed in the vertical velocity field, there were high-frequency (wavelength of less than 1 km), low-amplitude (~0.2 K) fluctuations in potential temperature likely caused by turbulent mixing.

The highest mixing ratios generally corresponded with the roll updrafts at all flight levels, suggesting that the rolls were transporting high surface moisture values upward and low stable-layer moisture values downward (e.g., LeMone 1973; Kristovich 1991). The largest amplitude CBL variations (~2 g kg^{-1}) occurred on scales of 2–5 km and were therefore likely caused by roll motions. The turbulent mixing of moisture, which caused variations of less than 0.5 g kg^{-1}, was evident at all levels but was most pronounced near the surface (Fig. 6b).

The flight track within the stable layer actually penetrated clouds (Fig. 6c). This was observed on both the in-flight video and the cloud liquid water field measured by the UW King Air. The times of the primary cloud penetrations, as determined from the cloud liquid water field (not shown), are indicated as schematically drawn clouds. The cloud penetrations corresponded with the maximum updrafts, moisture, and radar reflectivity, as well as relatively low potential temperatures. Beneath the clouds within the CBL (Fig. 6d) maxima were observed in reflectivity, vertical velocity, and mixing ratio. The higher-frequency variations of the potential temperature signal of Fig. 6d was likely due to turbulence.

The magnitude and frequency of the variability is more clearly seen with histograms. Figure 7 shows the distribution of the mixing ratio and potential temperature fields of the data shown in Fig. 6. For each day the left panels show the mixing ratio (Figs. 7a, 7c, 7e, and 7g), while the right panels (Figs. 7b, 7d, 7f, and 7h) show the potential temperature frequencies during the flight tracks. The scales for the horizontal axes are the same for all panels but the ranges are different for the stable-layer panels (Figs. 7e and 7f) since this flight experienced much warmer and drier conditions. Plotted

beneath each figure are the mean and standard deviation for the variable during the flight leg shown by the dot and solid line, respectively. The extended dashed lines on the mixing ratio panels signify the ranges of measurements observed. There had to be at least two occurrences of a measurement before it was included in this range. The sounding symbol shows the sounding's 200-m average value of that variable centered at the aircraft flight level. The cloud symbols will be described later.

The potential temperature within the CBL exhibited only about 0.5-K variability (Figs. 7b, 7d, and 7h). This is consistent with the difference in sounding potential temperature values when comparing a sounding launched within a roll updraft to one launched between an updraft and downdraft portion of rolls (Fig. 5), as well as with previous studies. The variability within the stable layer (Fig. 7f) was greater ($\sim$1 K).

The mixing ratio variations of 2.0–2.5 g kg^{-1} due to rolls, as compared with less than 0.5 g kg^{-1} due to turbulence (see Fig. 6), occurred at all flight levels within the CBL (Figs. 7a, 7c, and 7g). This magnitude is similar to that shown in the sounding comparison on 17 August (i.e., 1.5 g kg^{-1}; Fig. 5). Thus, with clear-air roll occurrences, moisture variabilities of 1.5–2.5 g kg^{-1} generally occurred throughout the CBL. Within the stable layer (Fig. 7e) the variability was even larger: 4.5 g kg^{-1}. The larger-amplitude perturbations of both potential temperature and mixing ratio within the stable layer were likely caused by entrainment between the relatively cool, moist CBL air and the relatively warm, dry stable-layer air.

Some skepticism may be induced since the magnitude of the moisture variations are of the same order as the absolute accuracy of the sounding measurements. This can be addressed with a comparison between the aircraft and sounding measurements shown in Fig. 7. For all four of the moisture panels shown in Fig. 7, the sounding values were within 1.4 standard deviations of the aircraft means, providing confidence for both measurements. The soundings often measured mixing ratio values of about 0.5 g kg^{-1} less than the aircraft means. This difference, however, is significantly less than the observed CBL moisture variability. In addition, both the aircraft and the soundings measured similar magnitudes of the variabilities.

It is not surprising that the thermodynamic variability due to the rolls was more significant in the moisture field than the thermal field. Mahrt (1976) found that the vertical temperature flux decreases with height more rapidly than the moisture flux since the vertical gradient of potential temperature is less than the vertical gradient of moisture. This is due to the fact that the thermal entrainment at the top of the CBL and the surface temperature flux both act to warm the CBL, causing a reduced vertical thermal gradient. The moisture flux, however, is such that the flux at the top of the CBL tends to dry the CBL, while the flux at the surface moistens the CBL, causing an enhanced vertical moisture gradient. Thus, the most pronounced thermodynamic transport due to rolls would occur with the moisture field.

The mixing ratio plots obtained within the CBL were typically negatively skewed; that is, the high mixing ratio values occurred more frequently than the low values (Figs. 7a, 7c, and 7g). The same was true for the vertical velocity field (not shown). This is suggestive of a vertically growing CBL with moist updrafts (1–3 m s^{-1}) dominating over dry downdrafts ($\sim$1 m s^{-1}), as is the case in the early afternoon in Florida. In fact, on 2 August the CBL depth increased from 1 km at 1600 to 1.2 km at 1650 to 1.3 km at 1800. On 10 August the CBL depth was 1.1 km at 1700 and 1.3 km at 1800. Within the stable layer there was a relatively equal number of high and low mixing ratio values (Fig. 7e); that is, neither the updrafts nor the downdrafts dominated.

The skewness of the histograms was compared with various theoretical functions (not shown). A negatively skewed distribution was obtained from a time series with relatively broad maxima and narrow minima. This is in agreement with the CBL time series, which showed that the aircraft were generally within the higher mixing ratio values longer than the lower mixing ratio values (e.g., Fig. 7a). A histogram similar to that within the stable layer (Fig. 7g) was produced using white noise. Thus, it is likely that the stable-layer histogram was depicting a preponderance of random turbulence.

5. Effect of moisture variability upon the expected cloud field

The soundings for 2 and 10 August are shown in Fig. 8. The launch locations are respectively shown in Figs. 4b and 4c. Schematic diagrams indicating the ascent positions relative to the roll circulations on both days are included. Just as in Fig. 7, the dots are the aircraft-measured means and the solid lines extend outward to one standard deviation. The dashed extensions are the entire ranges of mixing ratio values. The entire ranges are not shown for the potential temperature since the ranges were so small. There are four tracks (two for each aircraft) shown here, while only two tracks each were shown in Figs. 6 and 7. The extra tracks were added to the soundings to show that similar ranges were generally observed throughout the CBL. All data plotted were obtained from cross-roll flight tracks within 15 min of the sounding launch time.

The symbols CB_s indicate the lifting condensation levels (LCL) predicted by the soundings and were $1.1z_i$ (1300 m AGL) on 2 August and $1.2z_i$ (1336 m AGL) on 10 August. Cloud photographs were taken on these two days and were used to determine the observed cloud-base heights (CB_p) of $0.9z_i$ (1100 m AGL) on 2 August and $1.1z_i$ (1250 m AGL) on 10 August. On

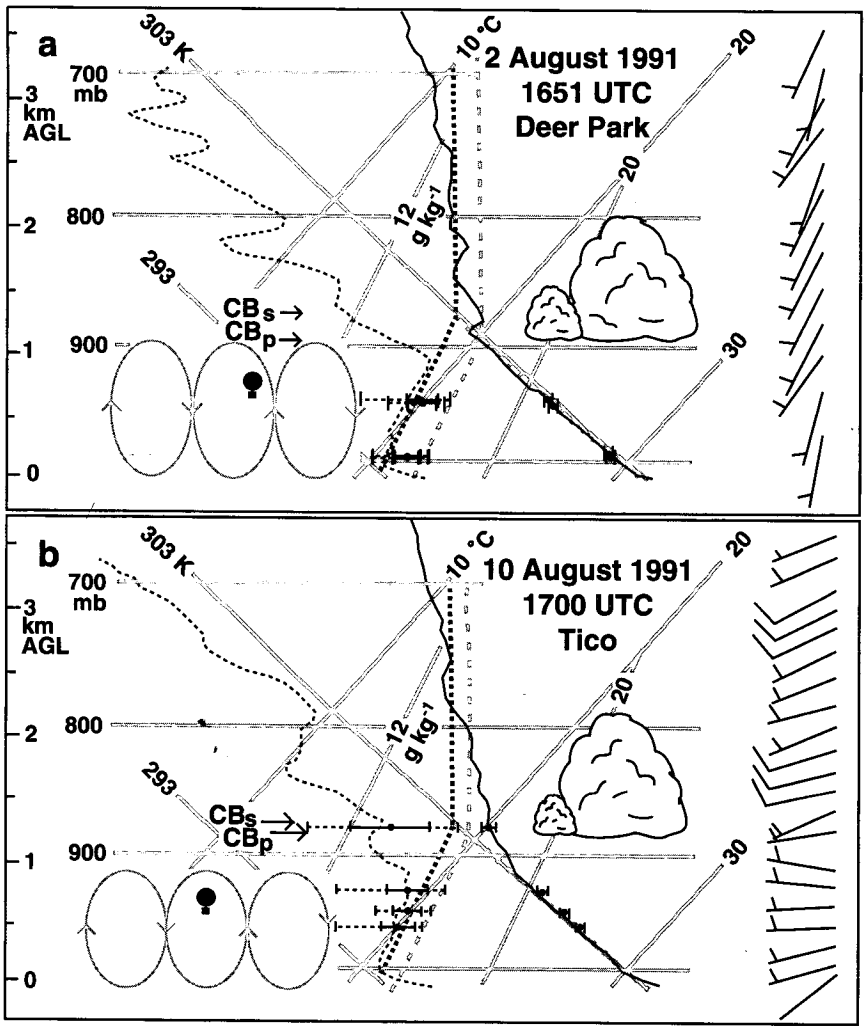

FIG. 8. CLASS soundings for (a) Deer Park at 1651 UTC 2 August and (b) Tico at 1700 UTC 10 August. Launch site locations are shown in Figs. 4b and 4c, respectively. Schematic diagrams illustrate the approximate launch locations relative to the roll circulations. The mean and standard deviations of aircraft-measured mixing ratio and potential temperature are respectively shown by the dot and solid lines at four heights. The entire ranges of mixing ratio values observed are shown by the dashed lines, as in Fig. 7. Cloud bases predicted by the sounding are labeled CB_s, while cloud bases measured from photographs are labeled CB_p. The schematic clouds represent the base and depth of clouds measured from the photographs. Parcel ascent tracks predicted by the soundings (black dashed lines) and expected from observed cloud bases (gray dashed lines) are shown. Wind barbs are the same as in Fig. 5.

2 August it was possible to determine cloud bases of three clouds on three different rolls, while on 10 August cloud bases of four clouds on three different rolls were measured. Thus, these cloud-base values represent average heights over the entire cumulus field, not simply the cloud base produced by one roll. Furthermore, the variability of all cloud bases measured from photogrammetry was less than 50 m. Since the 10 August UW King Air flight track at $1.15z_i$ (1269 m) was above cloud base, as discussed in section 4, this provides evidence that the sounding was predicting too high of an LCL and that the photogrammetric cloud base was supported.

For both cases, the LCL expected from the sounding was higher than that determined from photogrammetry. Since there was little CBL variability in potential temperature, mixing ratio variabilities were the likely cause of this discrepancy. On 2 August the sounding measured an average mixing ratio value of 15.5 g kg^{-1} in the lowest 50 mb, which combined with the potential temperature of 302.8 K to suggest a cloud base of $1.1z_i$. Using the same potential temperature of 302.8 K, in

order to obtain the observed cloud-base height of $0.9z_i$, a parcel mixing ratio value of 17.0 g kg^{-1} is required. On 10 August the sounding measured an average lowest 50-mb parcel mixing ratio value of 15.5 g kg^{-1} and parcel potential temperature of 303.1 K to suggest a cloud-base height of $1.2z_i$. Using the same potential temperature, a parcel mixing ratio value of 16.3 g kg^{-1} is required to produce the observed cloud-base height of $1.1z_i$. The respective mixing ratio values necessary to produce the observed cloud bases on 2 and 10 August (17.1 and 16.3 g kg^{-1}) were close to the surface mixing ratio values (17.2 and 16.6 g kg^{-1}). The values necessary to create cloud bases at heights determined by photogrammetry were shown by the cloud symbols of Fig. 7. The cloud symbols were not used for the 10 August $1.15z_i$ track since it was above cloud base (Figs. 7e and 7f). The mixing ratio values that created the observed cloud-base heights were within the range of measurements taken by the aircraft but consistently on the high end. The highest mixing ratio values were previously shown to coincide with roll updraft regions (Figs. 5 and 6). *Thus, the clouds were formed from the air parcels containing the relatively high mixing ratio values observed within the roll updraft regions.* It was therefore likely that those moist parcels of air, which determined LCLs as shown by photogrammetry, were also the most representative values to use in the prediction of the potential for deep, moist convection. The corresponding parcel ascent trajectories are shown by the gray dashed lines of the soundings (Fig. 8).

It may seem strange that the aircraft did not measure potential temperatures closer to 303.1 K (i.e., the parcel potential temperature) since it flew so close to cloud base at $1.15z_i$ (Fig. 8b). The difference between the aircraft minimum potential temperature value (303.3 K; see Fig. 7f) and the parcel potential temperature (303.1 K) is so small that it could be attributed to instrument error. The frequency of occurrence of 303.3-K potential temperature values, however, is very small. In addition, the aircraft-measured temperatures within cloud were likely too low due to wetting of the temperature sensor (e.g., Lenschow and Pennell 1974). The fact that the aircraft consistently measured values higher than the parcel potential temperature may be explained by the release of latent heat of condensation. Assuming that the formation of all of the cloud water measured by the aircraft ($\sim$0.11 g m^{-3}) contributed to latent heat release, the expected increase in temperature was approximately 0.25 K. Therefore, the potential temperature values measured by the aircraft were higher than the parcel values because it was often within the clouds that were warmed by latent heat release. The times at which the aircraft was not penetrating clouds, the potential temperatures were even slightly higher (see Fig. 6c). This may have been due to both the stable layer atop the CBL and subsidence warming caused by the small cumulus cloud motions.

The cloud-top heights were photogrammetrically measured on at least two different hard-based clouds each on 2 and 10 August. These ranges are shown by the vertical extent of the schematically drawn clouds of Fig. 8. It appears that each of the four cloud-top heights corresponded to small stable layers of the temperature profiles, suggesting that cloud growth may have been inhibited by the stable layers. It is also possible that detrainment at cloud top produced the stable layers. On 10 August, in particular, there was some indication that the cloud-top heights also corresponded well to reductions in moisture, implying that entrainment of relatively drier air may have reduced the potential for cloud growth.

The entire soundings for 2 and 10 August are shown in Fig. 9, along with tables comparing stability parameters assuming that soundings were launched in various portions of the rolls. The parameters listed are the lowest 50-mb average mixing ratio (g kg^{-1}) and potential temperature (K) used in the calculations of LCL, level of free convection (LFC), convective inhibition (CIN), lifted index (LI), and convective available potential energy (CAPE). Parcel 1 (P_1) is indicative of the minimum moisture observed by the aircraft within the CBL on each day. This likely occurred within the roll downdraft region, as shown schematically in the figure. Parcel 2 (P_2) represents the actual soundings. Parcel 3 (P_3) provides information for the maximum moisture values measured by the aircraft. This also generally corresponded with cloud-base measurements from photogrammetry. Thus, P_3 is likely the most representative of the potential for deep, moist convection. There was a large variation in the stability parameters depending upon which parcel trajectory was assumed. For example, on 10 August if the sounding were launched into the roll downdraft region (P_1) the predicted CAPE would have been 420 J kg^{-1}, but if it were launched into the roll updraft region (P_3) the predicted CAPE would have been 1684 J kg^{-1} (Fig. 9b). Thus, a CBL mixing ratio value of 2.3 g kg^{-1} higher produced a CAPE four times larger. Therefore, unless the sounding happened to be launched into the roll updraft region, it underestimated the convective potential.

Similar results were found in a numerical modeling study by Crook (1991), who showed that an increase in dewpoint temperature of 1–2 K could change a model forecast from null to the prediction of deep convection. Indeed, the corresponding dewpoint temperature variations in this study were 2–3 K, which produced significantly different sounding estimates of the potential for convective development.

6. Summary and conclusions

It has long been known that horizontal convective rolls affect the heat and moisture budget of the CBL. The resulting horizontal variability in temperature and moisture measurements throughout the entire CBL due

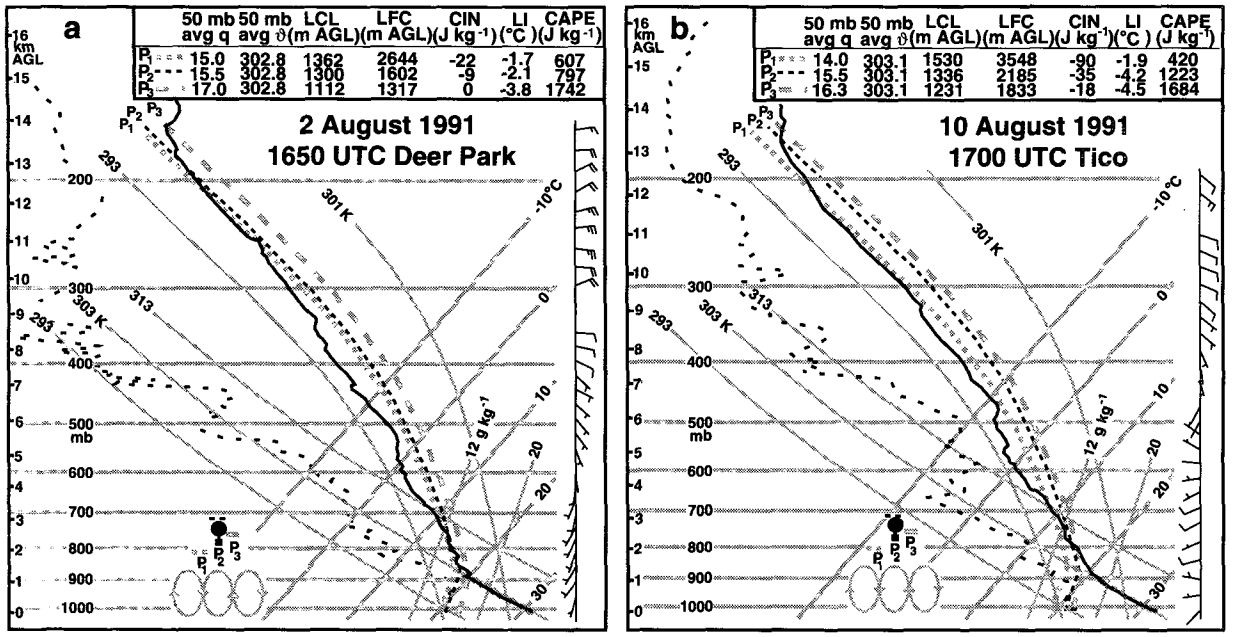

FIG. 9. Full soundings for (a) 1650 UTC 2 August of Fig. 8a and (b) 1700 UTC 10 August of Fig. 8b. Three parcel ascent tracks are shown to indicate the variations depending on low-level mixing ratio values. Parcel 1 (P_1) represents the minimum moisture measured by the aircraft, P_2 represents the parcel ascents expected from the soundings, and P_3 represents both the maximum moisture measured by the aircraft and the parcels producing cloud-base heights determined from photogrammetry. Tables showing stability parameters for the three parcel ascents are shown. Wind barbs are the same as in Fig. 5.

to clear-air rolls and how the variability influences the environment had not been previously examined in detail. To examine the CBL in the presence of rolls, two sounding comparisons were made: one within a roll updraft region and one between the updraft and downdraft portion of rolls. They showed an approximate 1.5 g kg^{-1} difference in the mixing ratio throughout the entire CBL. Aircraft data were added to provide further evidence that moisture variations of this magnitude were consistently found within the CBL and were caused by rolls. The updrafts observed by the aircraft corresponded with the enhanced radar reflectivity bands due to the rolls. In addition, the updrafts and enhanced reflectivity both agreed well with the maximum mixing ratio values at all levels. At low levels, in particular, the potential temperature maxima were in phase with the roll updrafts. Thus, the relatively warm, moist, surface-layer air was concentrated in the roll updraft regions as the rolls mixed the CBL air. The potential temperature variations due to rolls were only about 0.5 K, while the mixing ratio variations were 1.5–2.5 g kg^{-1} throughout the entire depth of the CBL.

It is well known that soundings give point measurements throughout their vertical ascents and may therefore not be representative of the environment (Stull 1988; Mueller et al. 1993). After using cloud photogrammetric techniques to determine the actual cloud-base heights, it was shown that the roll updraft air was most representative of the observed LCL. Thus, when rolls are present, sounding measurements are likely to underestimate the amount of moisture within the CBL unless the sounding happens to be launched into a roll updraft region. This is shown schematically in Fig. 10. Near the surface, the moisture field shows high-frequency variability and is not affected by the rolls. The clouds produced within the roll updraft regions are formed from the relatively moist air that originated at the surface and penetrated the CBL. The cloud bases produced with this relatively moist air are relatively low and the clouds are relatively deep (schematically shown by the solid cloud). This can be compared with cloud bases and depths that would be expected if moisture measurements directly beneath them were used to predict the stability parameters. The expected bases would be higher and the predicted cloud depths may be more shallow (shown by the dashed clouds in Fig. 10).

Results presented herein may have implications for both forecasters and cloud modelers. They require thermodynamic measurements from within the CBL to make their forecasts and run their simulations. If the measurements during roll occurrences are not taken within a roll updraft region, then it is likely that the moisture values will be too low and their predictions and simulations of the expected cloud field will be underestimated. Perhaps with the installation of NOAA's Wind Profiler Demonstration Network, many of which are equipped with the radio acoustic sounding system

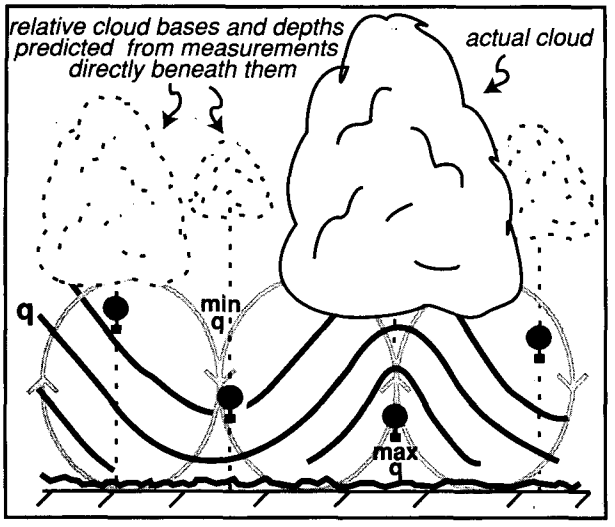

FIG. 10. Schematic diagram summarizing results of this study. Gray lines indicate roll circulations. Thick black lines are contours of moisture with the maxima existing within the roll updraft regions. Actual cloud base and depth are shown by the solid cloud. Dashed clouds represent relative cloud bases and depths expected if stability parameters were estimated from CBL moisture values directly beneath those clouds.

(RASS) capability to measure virtual temperature, it may be possible to use these results. Using moisture variations observed in this study, the corresponding variations in virtual temperature are 0.2–0.4 K. With a RASS continuously sampling the atmosphere as rolls propagate overhead, virtual temperature variations may be apparent since the typical absolute measurement error is 0.1–0.35 K (e.g., Martner et al. 1993; Angevine and Ecklund 1994). Assuming that the temperature variability is negligible, the RASS would allow for a continuous, detailed horizontal and vertical examination of the moisture variability due to rolls. It may also be possible to adjust the morning sounding with this information of the maximum moisture observed within roll updrafts to obtain more representative predictions and numerical simulations of the potential for deep, moist convection.

Acknowledgments. Discussions on this topic with Chuck Wade, Jim Fankhauser and Andrew Crook (all of NCAR) were extremely helpful. Nolan Atkins (UCLA) helped the first author while learning photogrammetric and satellite gridding techniques, as well as provided a detailed review of this manuscript. Thanks to Peggy LeMone (NCAR), two anonymous reviewers, and James Pinto (CU—Boulder) for providing in-depth reviews that improved this manuscript. All of the radar, sounding and surface station data were obtained from Bob Rilling (NCAR). Steve Williams (UCAR) provided the satellite imagery. The software package REORDER, written by Dick Oye and Michele Case (both of NCAR), was used to interpolate the radar data onto a Cartesian grid. Analyses and displays of the sounding and PAM II station data were respectively accomplished with SUDS and ROBOT. Both programs were written by Chris Burghart (NCAR). Erik Miller (NCAR) provided the software necessary to correct the CaPE soundings. Special thanks to the NCAR/ATD field support personnel who so expertly collected data during CaPE. Research results presented in this paper were partially supported by NSF under Grants ATM 9221951 and 9422499.

APPENDIX

CaPE Sounding Corrections

As discussed in section 2, corrections were made to the soundings to account for radiational heating and sensor lag (Miller and Riddle 1994). The sounding corrections were made for both temperature and moisture. Since the thermistor was located in a position that was easily ventilated upon launch, the radiational heating of the boom did not significantly affect the temperature measurements and the corrections were minute. The humidity sensor, however, had to overcome both radiational heating and sensor lag since the sensor was not readily ventilated upon launch (Cole 1993). Although detailed analyses of these errors were performed on the Tropical Oceans Global Atmosphere Coupled Ocean–Atmosphere Response Experiment dataset, it was recommended by Surface and Sounding Systems Facility (SSSF/NCAR) personnel that similar corrections be made for the CaPE soundings since the launch conditions were likely similar (i.e., strong solar heating and poor ventilation prior to launch).

An example of the corrections made to the moisture measurements is shown in Fig. A1. It is apparent that a correction of approximately 0.5 g kg^{-1} in mixing ra-

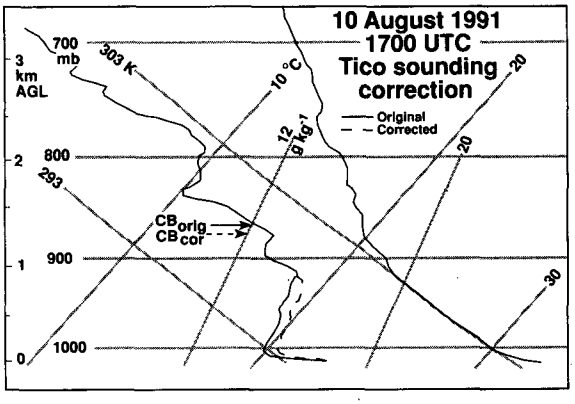

FIG. A1. Example of sounding correction from the Tico sounding at 1700 UTC 10 August 1991 shown in Fig. 8b. Corrections in the moisture profile (dashed line) were made to account for the radiational heating of the sensor and sensor lag. The corresponding corrected cloud-base height is shown by the dashed arrow.

tio was deemed necessary throughout the depth of the CBL for the Tico sounding at 1700 UTC 10 August 1991. This correction was based upon the collocated PAM measurements and the response time of the moisture sensor. This correction acted to decrease the sounding's predicted cloud-base height, which was then more comparable with the photogrammetric cloud-base height. If the corrections were not made, the CBL moisture measurements made by the soundings would have been more biased toward low values and the resulting estimates of the potential for deep moist convection would have been underestimated even more than those shown in this paper.

REFERENCES

Achtemeier, G. L., 1991: The use of insects as tracers for "clear-air" boundary-layer studies by Doppler radar. *J. Atmos. Oceanic Technol.*, **8,** 746–765.

Angevine, W. M., and W. L. Ecklund, 1994: Errors in radio acoustic sounding of temperature. *J. Atmos. Oceanic Technol.*, **11,** 837–842.

Asai, T., 1970: Three-dimensional features of thermal convection in a plane Couette flow. *J. Meteor. Soc. Japan,* **48,** 18–29.

——, 1972: Thermal instability of a shear flow turning the direction with height. *J. Meteor. Soc. Japan,* **50,** 525–532.

Atlas, D., S.-H. Chou, and W. P. Byerly, 1983: The influence of coastal shape on winter mesoscale air–sea interaction. *Mon. Wea. Rev.*, **111,** 245–252.

——, B. Walter, S.-H. Chou, and P. J. Sheu, 1986: The structure of the unstable marine boundary layer viewed by lidar and aircraft observations. *J. Atmos. Sci.*, **43,** 1301–1318.

Brown, R. A., 1980: Longitudinal instabilities and secondary flows in the planetary boundary layer: A review. *Rev. Geophys. Space Phys.*, **18,** 683–697.

Brümmer, B., 1985: Structure, dynamics and energetics of boundary layer rolls from KonTur aircraft observations. *Contrib. Atmos. Phys.*, **58,** 237–254.

Chou, S.-H., and M. P. Ferguson, 1991: Heat fluxes and roll circulations over the western Gulf Steam during an intense cold-air outbreak. *Bound.-Layer Meteor.*, **55,** 255–281.

Christian, T. W., and R. M. Wakimoto, 1989: The relationship between radar reflectivities and clouds associated with horizontal roll convection on 8 August 1982. *Mon. Wea. Rev.*, **117,** 1530–1544.

Clark, T. L., 1977: A small scale numerical model using a terrain following coordinate transformation. *J. Comput. Phys.*, **24,** 186–215.

Cole, H., 1993: TOGA COARE ISS radiosonde temperature and humidity sensor errors. NCAR Tech. Rep., 26 pp. [Available from Atmospheric Technology Division, NCAR, P.O. Box 3000, Boulder, CO 80307-3000.]

Cressman, G. P., 1959: An operational objective analysis scheme. *Mon. Wea. Rev.*, **87,** 367–374.

Crook, A., 1991: Small-scale moisture variability in the convective boundary layer and its implications for nowcasting. Preprints, *25th Conf. on Radar Meteor.*, Paris, France, Amer. Meteor. Soc., 67–70.

Deardorff, J. W., G. E. Willis, and B. H. Stockton, 1980: Laboratory studies of the entrainment zone of a convectively mixed layer. *J. Fluid Mech.*, **100,** 41–65.

Faller, A. J., 1965: Large eddies in the atmospheric boundary layer and their possible role in the formation of cloud rows. *J. Atmos. Sci.*, **23,** 466–480.

Fankhauser, J. C., C. J. Biter, C. G. Mohr, and R. L. Vaughan, 1985: Objective analysis of constant altitude aircraft measurements in thunderstorm inflow regions. *J. Atmos. Oceanic Technol.*, **2,** 157–170.

Grossman, R. L., 1982: An analysis of vertical velocity spectra obtained in the BOMEX fair-weather, trade-wind boundary layer. *Bound.-Layer Meteor.*, **23,** 323–357.

Holle, R. L., 1986: Photogrammetry of thunderstorms. *Thunderstorms: A Social and Technological Documentary,* Vol. 3, 2d ed., E. Kessler, Ed., University of Oklahoma Press, 77–98. [Available from the Superintendent of Documents, U.S. Government Printing Office, Washington, D.C. 20402.]

Kelly, R. D., 1982: A single Doppler radar study of horizontal-roll convection in a lake-effect snow storm. *J. Atmos. Sci.*, **39,** 1521–1531.

——, 1984: Horizontal roll and boundary-layer interrelationships observed over Lake Michigan. *J. Atmos. Sci.*, **41,** 1816–1826.

Kessinger, C. J., 1988: Operation and data summary for the Convection Initiation and Downburst Experiment (CINDE) held near Denver, Colorado from 22 June to 7 August 1987, 131 pp. [Available from Research Applications Program, NCAR, P.O. Box 3000, Boulder, CO 80307-3000.]

Kingsmill, D. E., and R. M. Wakimoto, 1991: Kinematic, dynamic, and thermodynamic analysis of a weakly sheared severe thunderstorm over northern Alabama. *Mon. Wea. Rev.*, **119,** 262–297.

Krishnamurti, R., 1975: On cellular cloud patterns. Part 1: Mathematical model. *J. Atmos. Sci.*, **32,** 1353–1363.

Kristovich, D. A. R., 1991: The three-dimensional flow fields of boundary layer rolls observed during lake-effect snow storms. Ph.D. thesis, The University of Chicago, 182 pp.

Kropfli, R. A., and N. M. Kohn, 1978: Persistent horizontal rolls in the urban mixed layer as revealed by dual-Doppler radar. *J. Appl. Meteor.*, **17,** 669–676.

Kuettner, J. P., 1959: The band structure of the atmosphere. *Tellus,* **2,** 267–294.

——, 1971: Cloud bands in the earth's atmosphere. *Tellus,* **23,** 404–425.

——, P. A. Hildebrand, and T. L. Clark, 1987: Convection waves: Observations of gravity wave systems over convectively active boundary layers. *Quart. J. Roy. Meteor. Soc.*, **113,** 445–467.

LeMone, M. A., 1973: The structure and dynamics of horizontal roll vortices in the planetary boundary layer. *J. Atmos. Sci.*, **30,** 1077–1091.

——, 1976: Modulation of turbulence energy by longitudinal rolls in an unstable planetary boundary layer. *J. Atmos. Sci.*, **33,** 1308–1320.

——, and W. T. Pennell, 1976: The relationship of trade wind cumulus distribution to subcloud layer fluxes and structure. *Mon. Wea. Rev.*, **104,** 524–539.

Lenschow, D. H., and W. T. Pennell, 1974: On the measurements of in-cloud and wet-bulb temperature from an aircraft. *Mon. Wea. Rev.*, **102,** 447–454.

Mahrt, L., 1976: Mixed layer moisture structure. *Mon. Wea. Rev.*, **104,** 1403–1407.

Malkus, J. S., and H. Riehl, 1964: Cloud structure and distributions over the tropical Pacific Ocean. *Tellus,* **16,** 275–287.

Martner, B. E., D. B. Wuertz, B. B. Stankov, R. G. Strauch, E. R. Westwater, K. S. Gage, W. L. Ecklund, C. L. Martin, and W. F. Dabberdt, 1993: An evaluation of wind profiler, RASS, and microwave radiometer performance. *Bull. Amer. Meteor. Soc.*, **74,** 599–613.

Miller, E. R., and A. C. Riddle, 1994: TOGA COARE integrated sounding system data Rep. Vol. 1A, 61 pp. [Available from Atmospheric Technology Division, NCAR, P.O. Box 3000, Boulder, CO 80307-3000.]

Moeng, C.-H., and P. P. Sullivan, 1994: A comparison of shear- and buoyancy-driven planetary boundary layer flows. *J. Atmos. Sci.*, **51,** 999–1022.

Mohr, C. G., and L. J. Miller, 1983: CEDRIC—A software package of Cartesian space editing, synthesis and display of radar fields under interactive control. Preprints, *21st Conf. on Radar Meteor.*, Edmonton, AB, Canada, Amer. Meteor. Soc., 569–574.

Mueller, C. K., J. W. Wilson, and N. A. Crook, 1993: The utility of sounding and mesonet data to nowcast thunderstorm initiation. *Wea. Forecasting,* **8,** 132–146.

Oye, R., and R. E. Carbone, 1981: Interactive Doppler editing software. Preprints, *20th Conf. on Radar Meteor.,* Boston, MA, Amer. Meteor. Soc., 683–689.

Palmén, E., and C. W. Newton, 1969: *Atmospheric Circulation Systems.* Academic Press, 603 pp.

Reinking, R. F., R. J. Doviak, and R. O. Gilmer, 1981: Clear-air roll vortices and turbulent motions as detected with an airborne gust probe and dual-Doppler radar. *J. Appl. Meteor.,* **20,** 678–685.

Rodi, A. R., J. C. Fankhauser, and R. L. Vaughan, 1991: Use of distance-measuring equipment (DME) for correcting biases in position, velocity and wind measurements from aircraft inertial navigation systems. *J. Atmos. Oceanic Technol.,* **8,** 827–834.

Stull, R. B., 1988: *An Introduction to Boundary Layer Meteorology.* Kluwer Academic Publishers, 666 pp.

Sun, W.-Y., 1978: Stability analysis of deep cloud streets. *J. Atmos. Sci.,* **35,** 466–483.

Sykes, R. I., and D. S. Henn, 1989: Large-eddy simulation of turbulent sheared convection. *J. Atmos. Sci.,* **46,** 1106–1118.

Wakimoto, R. M., and N. T. Atkins, 1994: Observations of the sea-breeze front during CaPE. Part I: Single-Doppler, satellite and cloud photogrammetry analysis. *Mon. Wea. Rev.,* **122,** 1092–1114.

Weston, K. J., 1980: An observational study of convective streets. *Tellus,* **32,** 433–438.

Wilson, J. W., G. B. Foote, N. A. Crook, J. C. Fankhauser, C. G. Wade, J. D. Tuttle, C. K. Mueller, and S. K. Krueger, 1992: The role of boundary-layer convergence zones and horizontal rolls in the initiation of thunderstorms: A case study. *Mon. Wea. Rev.,* **120,** 1785–1815.

——, T. M. Weckwerth, J. Vivekanandan, R. M. Wakimoto, and R. W. Russell, 1994: Boundary layer clear-air radar echoes: Origin of echoes and accuracy of derived winds. *J. Atmos. Oceanic Technol.,* **11,** 1184–1206.

Woodcock, A. H., 1942: Soaring over the open sea. *Sci. Mon.,* **55,** 226–232.